Study of vortex characteristics of a VATT wake based on CFD simulation

Zheng Yuan[1], WeiQi Liu[2], Liang Zhang*[3]

College of Shipbuilding Engineering, Harbin Engineering University, Harbin , China

[1]yuanzheng2016@ hrbeu.edu.cn

[2]liuweiqi@hrbeu.edu.cn

[3]zhangliang@hrbeu.edu.cn, Corresponding author.

Abstract— **The performance and array layout of the tidal turbine are closely related to wake flow and wake vortex characteristics. In this paper, the flow field of a 2D vertical axis tide turbine (VATT) model is simulated with CFD. The numerical simulation shows that the wake of VATT can be divided into 3 regions with different vortex characteristics. Compared the wake vortex characteristics with the different inflow velocity, the number of blades and the tip speed ratio (TSR), respectively, it found that the wake is significantly affected by the TSR. At the low TSR, the apparent blade stall makes the vortex distribution of near wake field very disorganized; at the optimal TSR, the wake field is relatively stable; at the high TSR, the distribution of the tail vortex in the far field obviously similar to the Kármán vortex street. The change regulation between the circulation and the TSR is found by monitoring the circulation of the shed vortex. The formula of the vortex motion trajectory is fitted by tracing the shed vortex with the tracer particles released from the trailing edge.**

Keywords— **VATT, tidal current energy, wake flow, wake vortex characteristics, CFD**

I. INTRODUCTION

An energy demands are soaring , the desire to explore alternate and renewable energy resources have become the focus on various active research. Tidal energy, a class of renewable energy, is attracting increasing interest as its spatial and temporal predictability and sizable potential. As the turbines trend to be arranged in an array layout, it is necessary to study the characteristics of the wake of the turbine. At present, there are many studies on the wake of horizontal axis tidal turbine(HATT), but there are relatively few researches on the wake of vertical axis tidal turbine(VATT), and the wake of VATT is more complicated. Therefore, it is necessary to study the characteristics of the wake of the VATT.

A momentum source term is added in the momentum conservation equation to study the HATT (Sun X et al. [1]). The added negative momentum source on a single dimension represents resistance, resulting in pressure steps and velocity losses. The thrust can be estimated by this method effectively, but there is no "double peak" phenomenon in the velocity distribution behind the plate. A porous disc was used to represent the HATT (Tedds SC et al. [2]), it was found that the anisotropic strength of the results are very weak due to the neglect of the rotation effect. Only the full-scale rotation model can simulate the rotation characteristic of the wake. A The numerical results were compared with the experimental results by Lam HF et al. [3], the numerical simulations of the 2D and 3D wakes of vertical axis wind turbines were conducted, the results show that, in the near wake region (within 3D), the speed loss is severe and the loss value can reach the maximum speed of 85%; in the far wake region (after 3D), the speed recover and reach the 75% of the maximum speed in the 10D position.

In this paper, the flow field of a 2D vertical axis tide turbine (VATT) model is simulated with CFD.

II. NOMENCLATURE

Tip speed ratio (TSR):

$$\lambda = \frac{\omega R}{U}$$

Solidity:

$$\sigma = \frac{Nc}{R}$$

Single blade tangential force coefficient and normal force coefficient:

$$C_{ft} = \frac{f_t}{0.5\rho U^2 cb} \quad , \quad C_{fn} = \frac{f_n}{0.5\rho U^2 cb}$$

Thrust coefficient and lateral force coefficient:

$$C_{F_X} = \frac{F_X}{0.5\rho U^2 cb} \quad , \quad C_{F_Y} = \frac{F_Y}{0.5\rho U^2 cb}$$

Power coefficient:

$$C_P = \frac{Q\omega}{0.5\rho U^3 cb}$$

Blade number: N
Blade chord length: c
Thickness of two-dimensional model: b
Torque: Q

III. CFD THEORY

Based on the theory of viscous hydrodynamics, the CFD method used to calculate the numerical change within a finite volume. The increase in fluid mass is equal to the net mass of fluid flowing into the microbody. According to this law, the mass conservation equation can be obtained, also known as the continuity equation:

$$\frac{\partial \rho}{\partial t} + \nabla \cdot (\rho \vec{u}) = 0$$

The method of time averaging is studied the pulsation of turbulence, which is the most widely use method. The turbulent motion is regarded as the sum of time-averaged flow and pulsating flow.

$$\frac{\partial \rho}{\partial t}+\frac{\partial}{\partial x_i}(\rho u_i)=0$$

$$\frac{\partial}{\partial t}(\rho u_i)+\frac{\partial}{\partial x_i}(\rho u_i u_j)=-\frac{\partial p}{\partial x_i}+\frac{\partial}{\partial x_j}\left(\mu\frac{\partial u_i}{\partial x_j}-\rho\overline{u_i'u_j'}\right)+S_i$$

From the control equation above, it can be seen there is one more item $-\rho\overline{u_i'u_j'}$ in the equation, which is defined as Reynolds Stress, it is expressed as $\tau_{ij}=-\rho\overline{u_i'u_j'}$.

IV. Model Geometry

The calculation domain setting is shown in the following figure. As the relatively good quality, structured mesh was refined the blade surface. To improve the accuracy of calculation, the thickness of the first layer is 0.1% of the chord length, the model is shown in Figure 2.

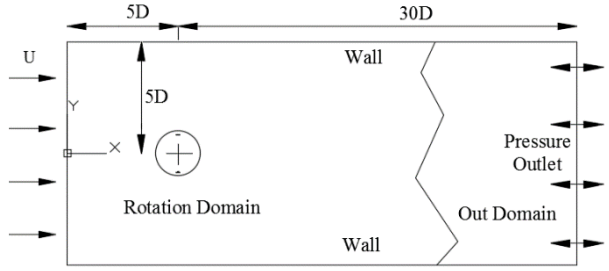

Fig.1 Domain and boundary conditions

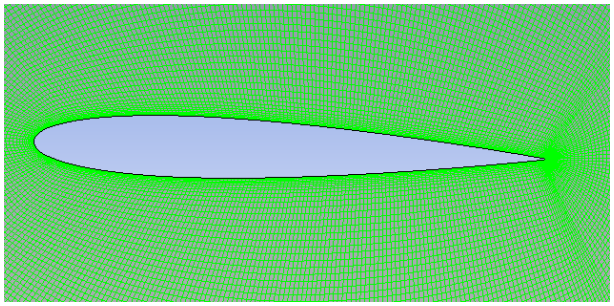

Fig.2 Detail of the prism layer around the airfoil

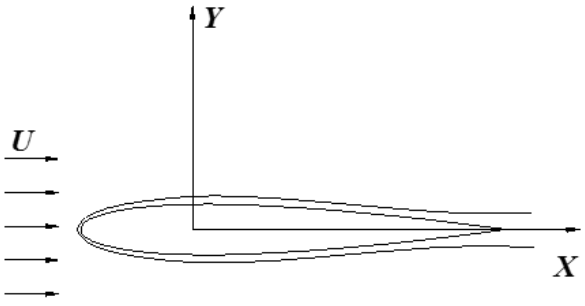

Fig.3 Reference coordinate system

V. Numerical Results and Discussions

A. Convergence study

The numerical model in this paper is validated by the classical experiment of Strickland [4], and the parameters of the VATT are shown in Table Ⅰ.

TABLE Ⅰ Parameters of the VATT

Parameters	value	unit
turbine diameter: D	1.22	m
Blade chord length: c	0.0914	m
span length: b	0.6	m
airfoil profile	NACA0012	
Blade number: Z	2	
Pitching angle	0	
Current velocity: U	0.091	m/s
Tip speed ratio (TSR): λ	5	

There are many results in the hydrodynamic performance calculation of VATT(e.g. [5]-[9]), referring to the relevant parameters setting, the parameters of this article are set as follows: The computational domain covers an area of 10D × 35D, the time step size, Δt, was set as $t=\pi/60\omega$ s, ensuring that the blade rotation angle is 3° at each time step, turbulence is modelled using the $SST\ k-\omega$ (shear stress transport) model.

The comparison between experiment and simulation of normal force coefficient and tangential force coefficient are shown in Figure 4. According to the graph, the trend of the two curves is similar, and there is the deviation at the vicinity of 180 and 360 degrees. Since the numerical model is a simplified two-dimensional model, ignoring the three-dimensional effect, the momentum transport in the Z direction was not considered, and the error was in an acceptable range. Therefore, it is illustrated that the numerical simulation method chosen in this paper has certain reliability.

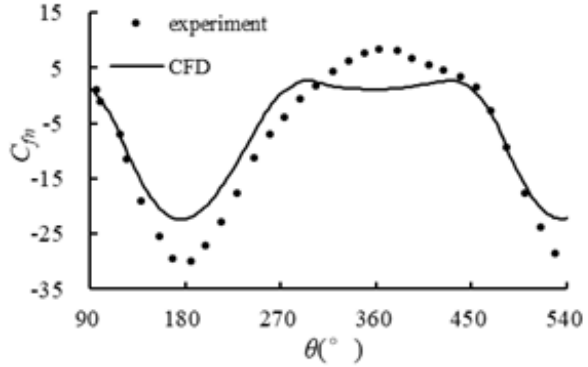

（a）normal force coefficient

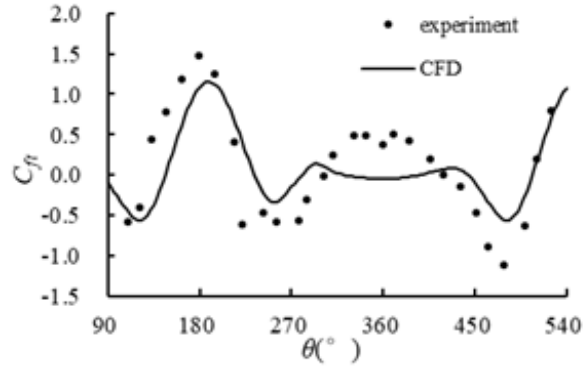

（b）tangential force coefficient

Fig.4 Comparison of the blade force

B. effect of different flow velocity

In this section, a single-blade turbine with a diameter of 1.2m and TSR of 5 is simulated. By changing the inflow velocity, the characteristics of vortex distribution in the wake of VATT can be found in the following diagrams. It is clear from the Figure 5 that when the tip speed ratio is fixed, the distribution of vortex in the near wake is similar, without significant change, as the inflow velocity increases.

So if the equivalent vortex model will be used to simplify the flow field, no matter how much the velocity is, as long as the TSR is the same, the wake field can be equivalent into one vortex model.

Figure 6 shows that the curves of the force coefficient are also consistent when the speed ratio is the same.

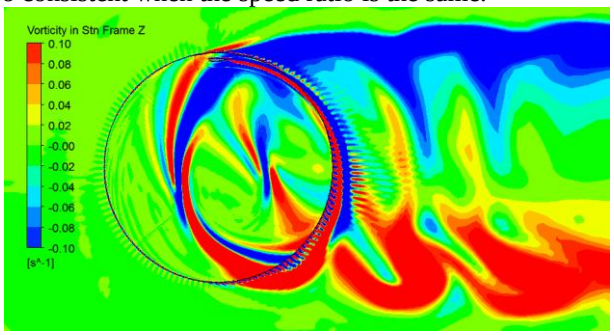

（a）U=0.1m/s

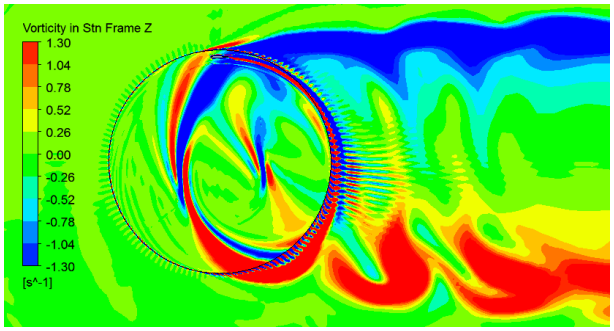

（b）U=1m/s

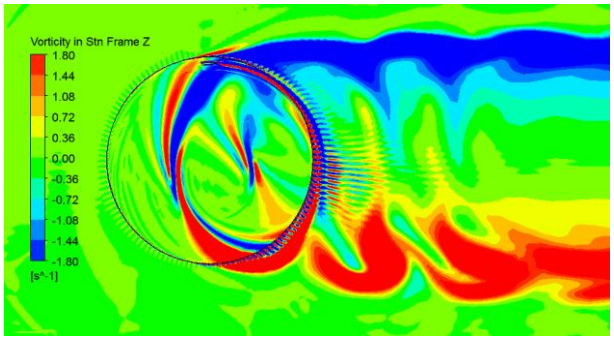

（c）U=1.5m/s

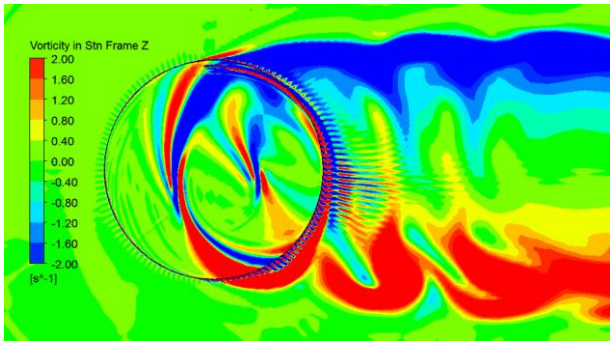

（d）U=2m/s

Fig.5 the vortex distribution in the near field at different inflow velocity

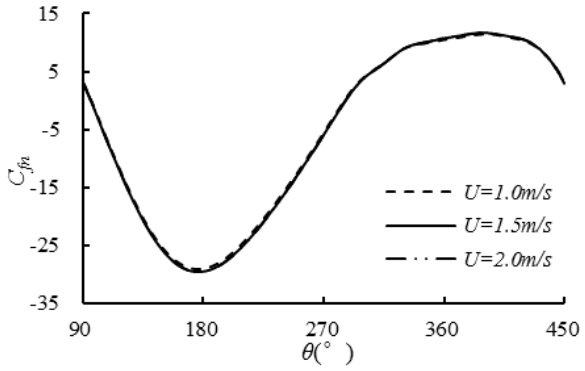

（a）normal force coefficient

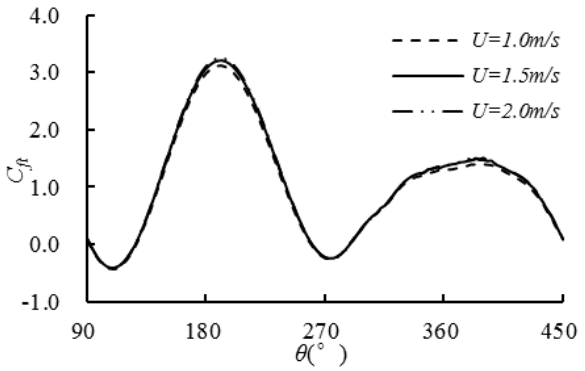

（b）tangential force coefficient

Fig.6 The blade force at different inflow velocity

C. effect of different tip speed ratio

Figure 7 shows the distribution of vortex at different speed ratios, and many differences can be found.

In the rotation domain, at the low speed of inflow, stall will be induced by big angle of attack in the upwind path. When the speed ratio increases, the stall phenomenon will disappear, but the frequency of blade passing through the vortex in the downwind path will increases, the problem of blade-vortex interaction (BVI) will be serious. Outside the rotation domain, the vortices do not fill the entire wake field, but are distributed in the upper and lower columns. Due to the vortex-vortex interaction(VVI), the shape of the vortex evolves from the initially generated strip to sphere.

Figure 8 shows the force curve at different speed ratios. when the azimuth angle between 90° and 270°, the normal force coefficient increases with the speed ratio decreases, but the tangential force coefficient shows the opposite trend. When the azimuth angle is in the range of 270° to 540°, the normal force coefficient changes little with the speed ratio. but the tangential force coefficient decreases as the speed ratio increases.

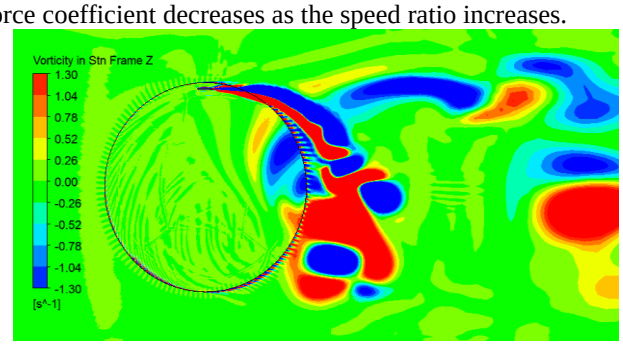

（a）TSR=2

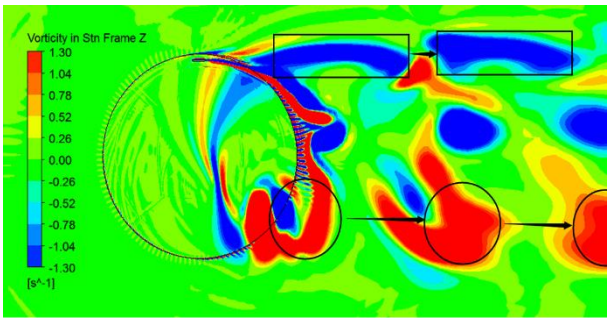

（b）TSR=3

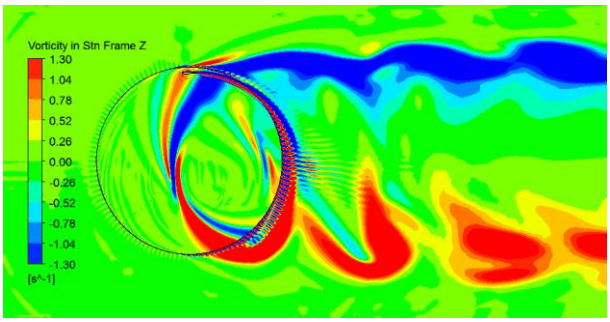

（c）TSR=4

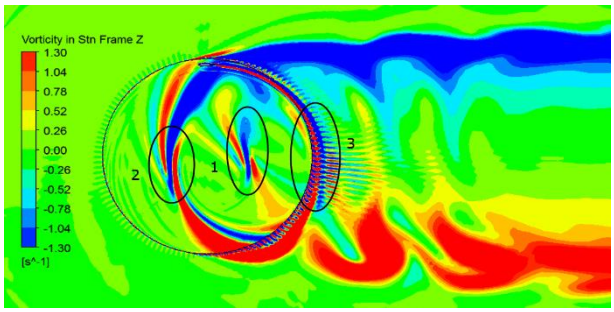

（d）TSR=5

Fig.7 the vortex distribution in the near field at different speed ratio

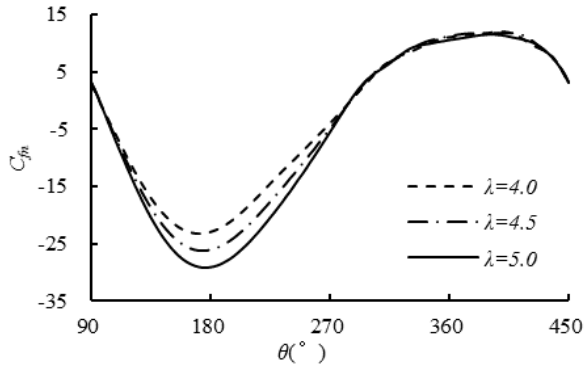

（a）normal force coefficient

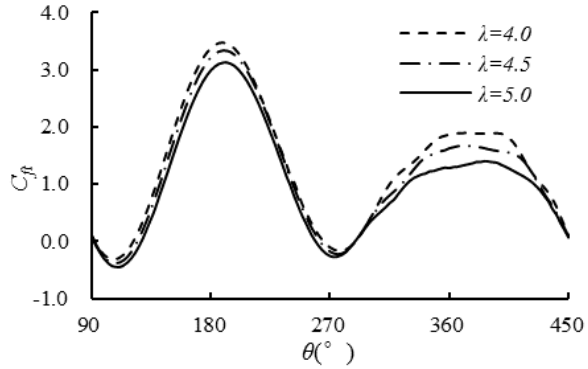

（b）tangential force coefficient

Fig.8 The blade force at different speed ratio

D. the Flow Field Partition

According to the morphology and characteristics of the vortex, the wake of VATT is divided into 3 regions：zone 1 and zone 2 and zone 3, as shown in Figure 9.

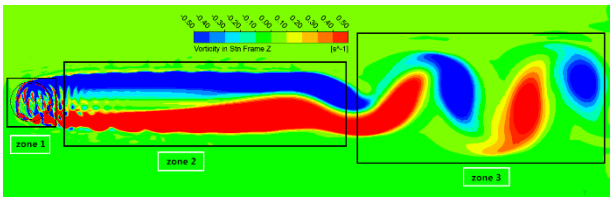

Fig.9 Schematic diagram of flow field partition

1) zone 1: In the turbine rotation domain where the vortex has just been generated. It is affected by the inflow, blade passing through, and another vortices interaction. The vortex structure is complex and the distribution is disordered.

2) zone 2: The vortices are distributed in the upper and lower columns. At this time, the vortex structure is relatively stable and will maintain a long distance, and the vortex train will show slight expansion and contraction in the cross-stream direction.

3) zone 3: In the far field of the turbine. The upper and lower columns of vortices began to lose the stability, showing significant convergence. During this process, the trail shows a "drift," which is similar to the Karman vortex street around a cylinder.

E. The difference in the far field

As described previously, the different speed ratios make a difference on the near field. Following to discuss the effect of different speed ratios on the far field. In order to discover the difference in far field more clearly, double blades were used to simulate in this section.

It can be seen from Figure 10 that the distribution characteristics of far-field vortices vary at different speed ratios. When the speed is relatively small, the angle of attack changes drastically, and it is prone to stall and generate a large number of high strength stall vortex, which leads to a disorderly distribution of vortex in the near wake region. In contrast, when the speed ratio increases, the vortex structure will be more stable. But when the speed ratio exceeds the optimum speed ratio, the position where the two rows of vortices merge in zone 3 gradually moves forward, and the wake will be more similar to the wake around the cylinder. Fig. 11 shows the vortex distribution of the two-bladed VATT at the high speed ratio (TSR 5.5), which is similar to the vortex distribution of flow around a circular cylinder in Fig. 12.

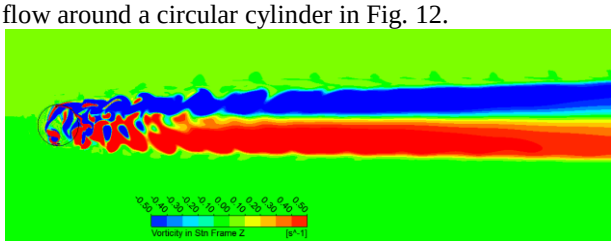

（a）TSR=2

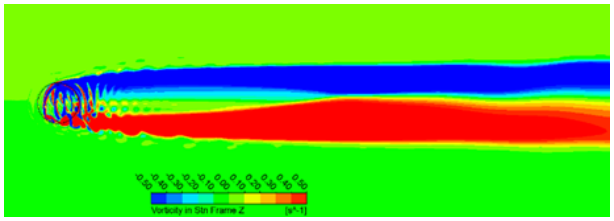

（b）TSR=3

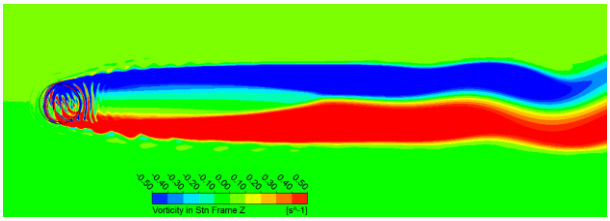

（c）TSR=3.5

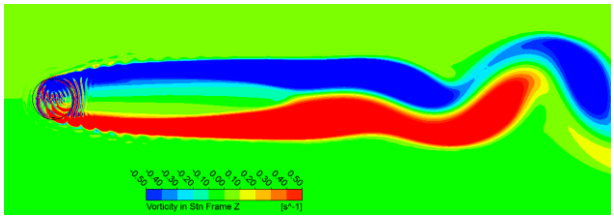

（d）TSR=4

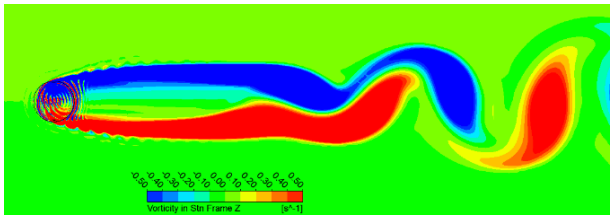

（e）TSR=4.5

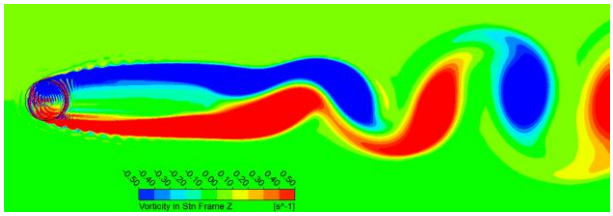

（f）TSR=5

Fig.10 the vortex distribution in the far field at different speed ratio

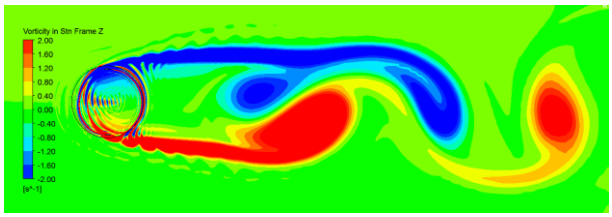

Fig.11 Flow field of a VATT

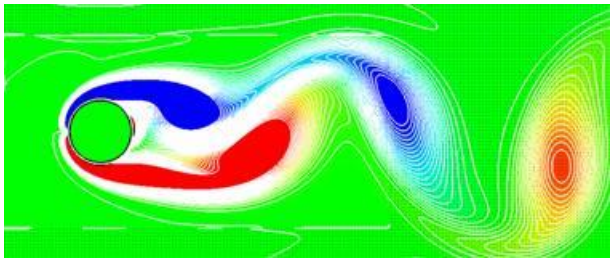

Fig.12 Flow field around a cylinder

F. unstable breakup of the wake

When the turbine speed is relatively low (speed ratio 2), there is an obvious speed loss zone behind the VATT, and the vortex is distributed in two columns. However, prolonging the simulation time, it can be found that an unstable breakup will occur in the wake, as shown in Fig. 13 and Fig. 14. Although the wake area becomes shorter, it will “grow” again and become longer, and this breakup phenomenon may occur again because of vortex instability. In the real 3D wake, due to the three-dimensional flow in the spanwise direction and higher turbulence (in this article, the turbulence intensity is 1%), the breakup phenomenon may not occur.

When designing the layout of the VATT, it is necessary to consider the influence of the wake of the turbine in the upstream. However, further studies are needed to be done on this phenomenon.

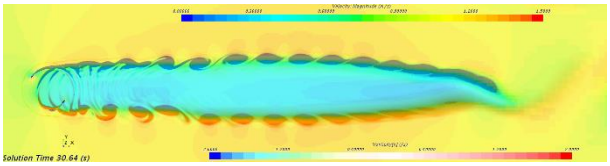

Fig.13 The wake of a VATT is going to break

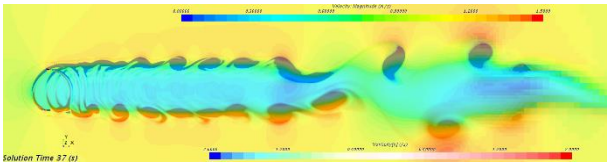

Fig.14 The wake of a VATT has broken

VI. CONCLUSIONS

The wake characteristics of VATT need to be studied in detail for the array layout and performance improvement of turbines. In this paper, the reliability of numerical simulation is verified by comparison with an experiment. Then, the characteristics of wake at different inflow velocities and different speed ratios are analyzed, and the wake is divided into three zones according to the characteristics of vortex distribution. The results show that the Zone 2 will be shorter at the higher speed ratio. It is also found that the unstable breakup phenomenon of VATT wake. By analyzing these characteristics, it will lay a foundation for the simplification of the VATT flow field in the future.

ACKNOWLEDGMENT

This work is supported by the Doctoral Scientific Fund Project of the Ministry of Education (no. P012213003). It is also supported by China-UK (NSFC-EPSRC/NERC) international collaborative research project (no. 5171101175), by NSFC projects (no. 11572094) and by the Fundamental Research Funds for the Central Universities (no. HEUCFP201809). This paper is funded by the International Exchange Program of Harbin Engineering University for Innovation-oriented Talents Cultivation.

REFERENCES

[1] Sun X, Chick J P, Bryden I G. Laboratory-scale simulation of energy extraction from tidal currents [J]. Renewable Energy, 2008, 33(6):1267-1274.

[2] Tedds S C, Owen I, Poole R J. Near-wake characteristics of a model horizontal axis tidal stream turbine [J]. Renewable Energy, 2014, 63(1-2):222-235.

[3] Lam H F, Peng H Y. Study of wake characteristics of a vertical axis wind turbine by two- and three-dimensional computational fluid dynamics simulations [J]. Renewable Energy, 2016, 90:386-398.

[4] Strickland J H, Webster B T, Nguyen T. A Vortex Model of the Darrieus Turbine: An Analytical and Experimental Study[J]. Journal of Fluids Engineering, 1980, 80(4):500-505.

[5] Wang Kai, Sun Ke, Sheng Qi-hu, Zhang Liang,Wang Shu-qi .The effects of yawing motion with different frequencies on the hydrodynamic performance of floating vertical-axis tidal current turbines. Applied ocean research.2016 ,59(9):224-235.

[6] Zhang XW, Wang SQ, Zhang L, et al. The hydrodynamic characteristics of free variable-pitch vertical axis tidal turbine [J], J of Hydrodynamics, 2012, 24(6): 834-839.

[7] WANG SJ. ZHAO LW, LI D, et al. Numerical Simulation on hydrodynamic performance of flexible blade turbine driven by tidal energy [J]. Acta Energiae Solaris Sinica, 2011, 3(3): 281-287.

[8] Lam HF, Peng HY. Study of wake characteristics of a vertical axis wind turbine by two- and three-dimensional computational fluid dynamics simulations, Renewable Energ [J]. 2016 (90): 386-98.

[9] Li Ye, Calisal SM. Numerical analysis of the characteristics of vertical axis tidal current turbines [J].Renewable Energy, 2010, 35 (2): 435– 442.